CIRP Journal of Manufacturing Science and Technology 17 (2017) 71–79

Contents lists available at ScienceDirect

CIRP Journal of Manufacturing Science and Technology

journal homepage: www.elsevier.com/locate/cirpj

The detection of wind turbine shaft misalignment using temperature monitoring

Oliver Tonks, Qing Wang *

School of Engineering, Computing Sciences, Durham University, DH1 3LE, UK

ARTICLE INFO

Article history:
Available online 31 May 2016

Keywords:
Couplings
Shaft misalignment
Condition monitoring
Temperature

ABSTRACT

Temperature is a parameter increasingly monitored in wind turbine systems. This paper details a potential temperature monitoring technique for use on shaft couplings. Such condition monitoring methods aid fault detection in other areas of wind turbines. However, application to shaft couplings has not previously been widely researched.

A novel temperature measurement technique is outlined, using an infra-red thermometer which can be applied to online condition monitoring. The method was validated and investigated through real time shaft alignment tests. Different modes of misalignment including offset and angular were investigated. This allowed analysis of the relationship between a change in shaft alignment and a change in temperature. The rate of change was found to be a factor of condition through exploring changes in ambient and operating temperatures. The test rig allowed quantification on a small scale and potential causes and effects of temperature changes are discussed.

Introduction

Wind energy is the most common renewable generation and has great potential to make important contributions towards the EU's renewables targets for 2020 [1]. More than 5000 turbines are operational in the UK and can produce approximately 10.5 GW of the UK's electricity supply [2]. The European Wind Energy Association (EWEA) forecasts that the percentage of turbine investment in offshore sites will rise from 25% in 2015 to about 60% in 2030 [3].

Offshore wind farms are increasingly popular since a greater number of larger turbines can capture the vast resource. These turbines utilise higher and more consistent wind speeds up to 17 m/s but experience greater failure rates [4–7]. Exposure to extreme ambient conditions in remote locations creates challenges for operation and maintenance [8]. Minor reliability issues can severely reduce availability because of difficulties associated with access in harsher environments [9]. In some cases a whole farm may be inaccessible for days at a time [8,10]. Routine servicing may be difficult, even given favourable weather due to factors such as distance offshore and site exposure [10]. Operation and maintenance incurs costs of between 25% and 30% of the capital cost [11,12]. This is almost the same cost compared with onshore [13].

Maintenance procedures play a key part in reducing unplanned downtime, in turn improving availability and useful life. Predictive maintenance is an area of significant development using online monitoring, such as the method devised, to determine the condition of components. The continual measuring of physical parameters incorporates a Supervisory Control and Data Acquisition (SCADA) System to give constant feedback on the state of the machine [14].

Changes in system behaviour can indicate root causes and in turn pre-empt larger faults. This provides advance warning of impending failure allowing the machine to be taken offline for repair [15]. This earlier detection reduces the cost of repair since less damage to a component is caused. The savings however, must outweigh the monitoring cost. An estimate of the figure spent on monitoring should be 5% of the capital value [15].

As the amount of generation from wind power increases, developments in terms of reliability and maintenance are necessary to reduce capital and operational costs. This research studies a technique to assist with maintenance – the online monitoring of temperature for shaft alignment detection. Particular focus is paid to couplings with misalignment identified as a potential failure mode. Monitoring the shaft misalignment is of

* Corresponding author. Tel.: +44 191 334 2381; fax: +44 191 3342408.
E-mail addresses: oliver.p.tonks@gmail.com (O. Tonks), qing.wang@durham.ac.uk (Q. Wang).

http://dx.doi.org/10.1016/j.cirpj.2016.05.001
1755-5817/

interest for several reasons. Firstly, during the manufacturing process, a misalignment monitoring system can be used to assure compliance with quality standards. Secondly, a shaft misalignment monitoring system provides temperature information in real-time, enabling very early warning in the case of abnormal heating of the shaft, thus preventing catastrophic failures and related production loses. It also provides information for condition-based maintenance of the shaft as part of the entire drivetrain. Furthermore, the analysis underlying the design of a monitoring system can yield hard limits on the physical capabilities of the shaft and hence improve the reliability of a wind turbine system to perform a more demanding task.

Misalignment

Monitoring methods are used to find root causes and identify potential causality [8]. The root cause considered in this research is that of shaft misalignment. This change in shaft position occurs due to non-co-linear shafts. The centre lines of coupled shafts should be parallel and intersect like a single shaft. The investigated modes of shaft misalignment are shown in Fig. 1, consisting of a mixture of offset (shafts on two separate, parallel centerlines) and angular (coaxial shafts at an angle) [16].

A wind turbine uses shafts to transmit power and motion from the rotor to the generator. For long term reliable and optimal running, acceptable alignment is required. Misalignment is a common problem, the cause of 30% of downtime [17]. The torque on the system at shutdown can cause this misalignment between shafts and components.

Should large misalignment arise from variable shaft loading [18] or torque imbalance, the eccentric running creates high frequency vibration [19,20]. This increases axial and radial loading on components, increasing fatigue damage. Damage to larger components and sub-assemblies such as generators are more costly and time consuming to maintain.

This indicates the importance of condition monitoring, with vibration techniques the first to be used initially on generators, gearboxes and bearings [10]. Instruments used include transducers, strain gauges [21] and optical encoders [22]. Misalignment can also be measured in terms of distance. Different indicator methods are used including laser based measurement, utilising the high accuracy and noncontact nature for online capture of misalignment [23,24].

Couplings

Failure mode, effect and criticality analysis (FMECA) is used to identify lesser reliable components and their failure modes. Misalignment, the failure mode outlined, impacts upon shaft couplings. Little research exists into coupling failures themselves. They are mainly categorised as brake and or/drivetrain failures. Brake failures account for 4% and the drivetrain as much as 17% of all failures [25]. These components have a cumulative annual failure rate of approximately 0.25 with between 3 and 9 days downtime required for repair [26].

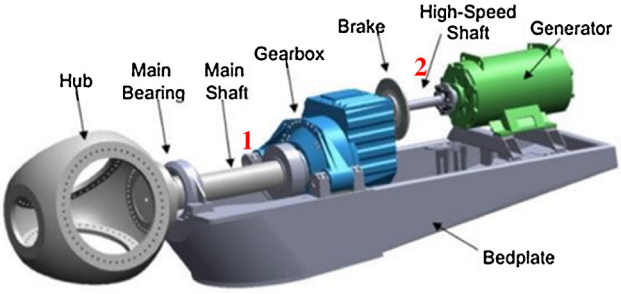

Fig. 2. Typical drivetrain layout.

Primarily, couplings are used to mesh driving and driven shafts together enabling rotational power transfer. In addition they tolerate and accommodate a degree of misalignment between these shafts. For example, Siemens Flender couplings cope with 20 mm in radial and axial directions [27]. In wind turbines couplings are likely to be used in two places, shown in Fig. 2: (1) between the low speed shaft and the gearbox and (2) between the gearbox output shaft and the generator, usually incorporating the brake [28].

Fig. 2 shows a typical drivetrain layout [29]. The generator is usually offset from the gearbox due to the gear arrangements and to allow access to the brake for maintenance. This offset increases the likelihood of misalignment so a coupling can be used in position 2 to counteract this.

Couplings are chosen based on various requirements such as stiffness, vibration and environment. There are two main types of coupling, rigid or flexible. Flexible elastomeric couplings are more appropriate in wind turbines given their high torsional softness enabling cushioning of shock and vibratory loads [30]. One common type of flexible coupling is double cardan, gaining flexibility by means of arrangement of two links [8]. Large values of misalignment can be accommodated with additional maintenance benefits arising since individual links rather than the whole coupling can be replaced.

Heat generation due to temperature rise

In a wind turbine system, the shaft is supported by bearings. The shaft rotation creates friction in the bearing elements which generates heat. The heat generation will increase if the torque due to shaft misalignment increases. By monitoring the temperature rise at the couplings, the degree of misalignment in the shaft system can be detected [31].

According to the first law of thermodynamics [32], for a specified torque, the work done during n revolutions is determined by

$$T = F_r = \frac{T}{r} \tag{1}$$

where the force acts through a distance S, which is related to the radius r by

$$s = 2\pi r n \tag{2}$$

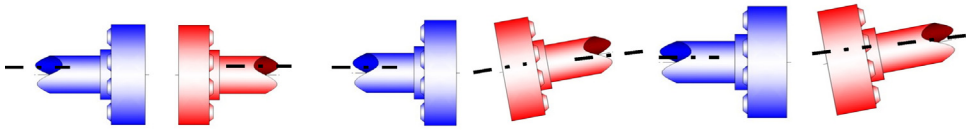

Fig. 1. Types of misalignment: (a) offset, (b) angular and (c) combination of both.

The shaft work is then determined from

$$W_s = F_s = 2\pi nT \tag{3}$$

The energy generated is the shaft work done per unit time, which is given by Eq. (4).

$$W_s = Q_\cdot = 2\pi Tn_\cdot \tag{4}$$

Consequently the heat is transferred by conduction from its surface to its surroundings. To determine the time dependence of the temperature distribution of the couplings during a transient process, a lumped capacitance method [33] has been used under the condition that the temperature gradients within the couplings are small. The rate of heat loss of the shaft rotation is proportional to the difference in temperature between the shaft (couplings) and its surroundings. This temperature-difference behaviour can be expressed by the Newton law of cooling as:

$$\frac{dQ}{dt} = h_\cdot A(T(t) - T_{env}) = h_\cdot A\Delta T(t) \tag{5}$$

where Q is the thermal energy, h is the heat transfer coefficient, A is the temperature of the object's surface and interior, T_{env} is the temperature of the environment, $\Delta T(t)$ is the time dependent thermal gradient between environment and object.

Temperature monitoring

Some vibration-based monitoring techniques are deemed unsatisfactory due to the variable nature and dynamic range creating false alarms [34]. Temperature monitoring is increasingly used within condition based maintenance and is the focus of this paper.

Increased loading due to misalignment causes a temperature rise [35]. Should this rise exceed the capability of a component then thermal expansion can arise through overheating [18]. This reduces operating clearances on couplings, increasing wear. A temperature monitoring method does not directly detect the failure or cause but provides an indication of a potential fault.

Commonly there are three approaches to temperature monitoring [36]:

1. Measure local point temperatures using surface or embedded temperature detectors.
2. Monitor the temperature of a larger area of the machine using thermal imaging.
3. Measure the temperature distribution of the machine or bulk temperatures of fluids.

The main difficulty is the conflict between easily made point measurements, giving only local information – due to the embedded nature of the measurement device – and more difficult bulk measurements which run the risk of overlooking local hot-spots [36].

Temperature is currently monitored on a variety of components within wind turbine systems. The temperatures of oil, bearings and generator windings are commonly measured using surface or embedded resistance temperature probes. In addition, the nacelle and ambient temperatures are monitored using fixed transducers which also measure parameters such as humidity and wind speed.

Techniques and sensors have developed over time through improvements in reliability, accuracy and response time allowing temperature measurements to be taken closer to the active parts of a machine [15]. Infra-red thermography is a non-contact technique allowing hot spot measurements from a distance as proposed in [37] and [38]. The method outlined in this research uses an infra-red thermometer to measure the surface temperature of a coupling by collecting emitted, reflected and transmitted energy.

Test rig

An existing test rig enabled real-time shaft alignment tests to be carried out. The rig shown in Fig. 3 uses a ∅6 mm shaft to connect the main components together. A DC motor was used to create shaft rotation, replicating the motion of a wind turbine blade hub. The two flexible double loop couplings were the focus of temperature measurement. Two types of misalignment were conducted to test radial misalignment and axial angular misalignment, as set out in Fig. 1(a) and (b). The system is given support by three deep groove ball bearings. One is fixed with the other two attached to lead screws to enable the creation of misalignment. Rotation of lead screw one (LS1) created offset misalignment and angular misalignment was created using lead screw two (LS2).

An infrared thermometer was used to measure coupling temperature during operation. This noncontact method was

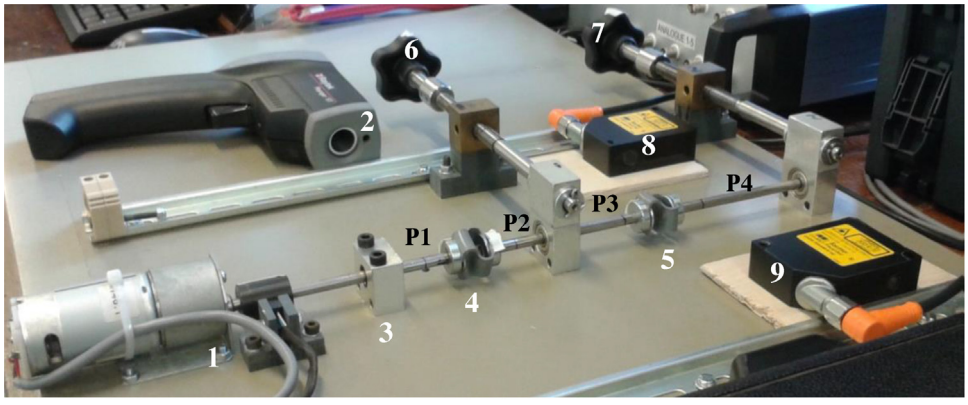

1-DC Motor 2-Infrared Thermometer 3-Fixed Bearing 4-Coupling1 5-Coupling2 6-Lead Screw1 with bearing 7-Lead Screw2 with Bearing 8-Left Measurement Laser 9-Right Measurement Laser

Fig. 3. Test rig.

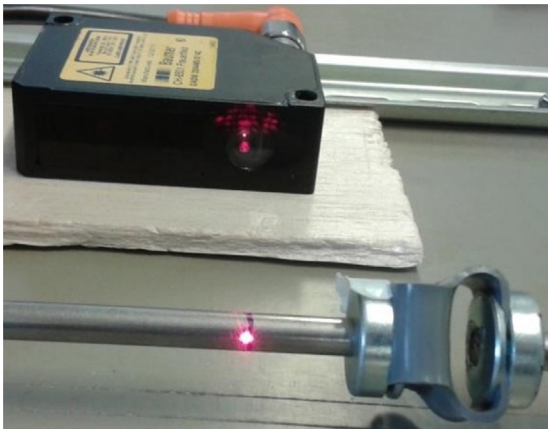

Fig. 4. Laser distance measurement.

appropriate due to the rotational nature of the rig. The display resolution of 0.2 °C is accurate to ±2 °C for temperatures up to 23 °C and ±1 °C above this. Even though the response time was 500 ms, the measurement was taken over a period of 5–10 s allowing any fluctuations to stabilise.

The misalignment value was quantified in terms of displacement using laser measurement, one of the most common methods in industry. The two Baumer Photoelectric Distance Measurement Devices are suitable for a rig of this scale to a measurement range of 30–130 mm, resolution of <0.07 mm and response time of <10 ms. This non-contact method shown in Fig. 4 was carried out online, whilst the shaft was rotating to also enable speed measurement. There are four measurement points along the shaft. As can be seen in Fig. 3, P1 and P2 are on either side of coupling 1, and P3 and P4 are on either side of coupling 2. The value of misalignment at positions P1–P4 was the difference between the starting and finishing value, the distance from the shaft to each of the lasers. Perfect alignment was a reference value at each position, monitored to ensure each repetition had the same amount of misalignment.

Experiment plan

Misalignment was artificially created for different experiments as follows:

1. LS1 3 rotations anti-clockwise (offset measured at 1.46 mm).
2. LS2 3 rotations clockwise (offset measured at 0.57 mm).
3. LS1 3 rotations anti-clockwise and LS2 3 rotations anti-clockwise (offset measured at 2.36 mm).
4. LS1 3 rotations anti-clockwise and LS2 3 rotations clockwise (offset measured at 1.18 mm).
5. The four previous experiments with gradually increasing misalignment (0–5 rotations).

These modes of misalignment are shown in Fig. 5, with numbers corresponding to the relevant experiment. The lead screws are set up in opposite directions. To move the particular bearing towards the left laser, lead screw one (LS1) required an anticlockwise rotation and lead screw 2 (LS2) a clockwise movement.

For the first four experiments, the effect of the type of misalignment on each coupling was found. Both couplings were measured in successive experimental runs and using these results, the most appropriate coupling for monitoring in experiment 5 was chosen.

Method

Using the test rig, a novel temperature measurement technique to enable online condition monitoring was designed. The position of measurement corresponds to the coupling midpoint seen in Fig. 6. Offline scanning found this to be the hottest point, the point of greatest loading on the coupling. The thermometer's distance to spot ratio was 12:1 so at 145 mm, the temperature was averaged in a 12 mm diameter area. The midpoint in this area corresponds to the laser sight, assisting with aiming.

The same procedure was followed for each of the first four experiments. Each run lasted 30 min and was split into three sections:

1. Initially the rig was aligned for 10 min.
2. Misalignment was created for the particular experiment and followed by another 10 min period.
3. Rotation was reversed to realign the shaft for a final 10 min.

This varying run was compared with entirely aligned and misaligned 30 min runs. Temperature monitoring was at 2 min intervals, as well as before and after to compare online and offline temperatures. Resting the thermometer on its side ensured it was level, in the same location and at the same angle for each experiment. The motor speed was also a constant variable, enabling direct comparisons between experiments.

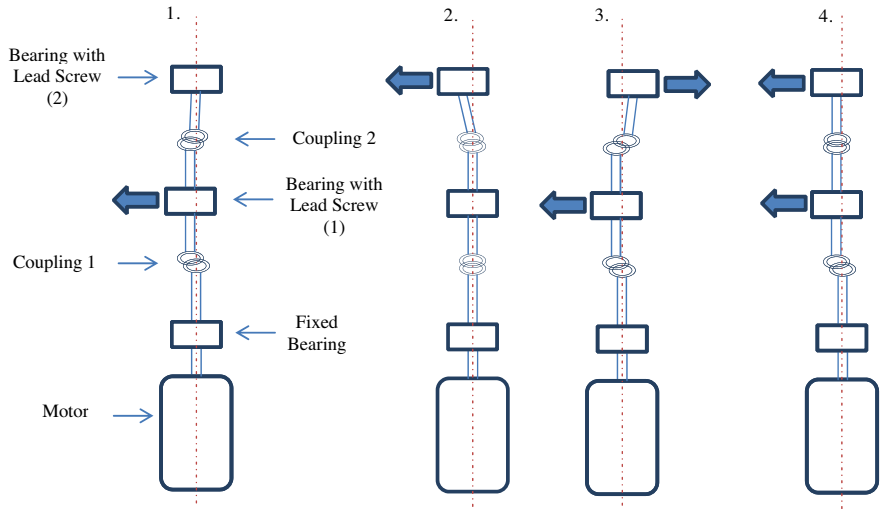

Fig. 5. Misalignment mode diagrams.

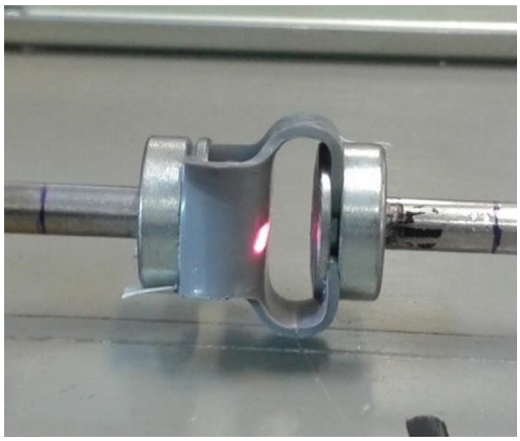

Fig. 6. Temperature measurement.

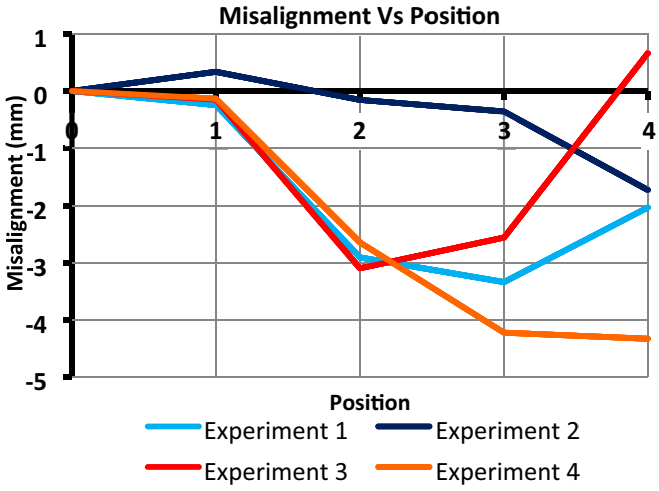

Fig. 7. Misalignment against position (left laser).

A 30 min period was also used for the fifth experiment. The shaft was increasingly misaligned by one rotation every 5 min. During this gradually worsening alignment, measurements of temperature were taken every minute.

Preliminary investigations

Preliminary experiments enabled the experimental plan and method to be verified. Temperature was found to be identical from either side of the coupling and a change in distance to the coupling caused no fluctuation.

Misalignment was always created in one direction (towards the left laser) since the difference in results when creating the four modes of misalignment in the opposite direction (away from the left laser) was negligible. The research aim was to view temperature change due to misalignment only so to monitor any changes in ambient temperature a standard wall thermometer was used for comparison throughout.

The stabilising time to reach normal operating conditions meant a short period of pre experimental running was introduced to avoid sharp increases. The time for temperature to stabilise due to a change in alignment was less than 10 min, validating the length of experimental runs.

Data analysis

As well as temperature investigations, the values of rotational speed and misalignment were monitored. These measurements were for reference purposes and not investigated. Since these parameters are constant, direct comparisons between the modes of misalignment were made.

Misalignment

Misalignment was measured to quantify the lead screw rotation and also ensured the amount was identical for each experimental repetition. Measurements were obtained using a data acquisition system designed in previous work [38]. The two lasers were connected through a National Instruments USB-6218 module and compatibility with DAQmx Drivers allowed software development in LabVIEW 2012. The sampling time of the laser was 10 ms, so to avoid issues associated with Nyquist's theorem, the data was sampled at 1000 Hz where 100 samples gave 0.1 seconds of data. For each experiment, Positions 1–4 were measured twice and averaged. These values are shown in Fig. 7. This figure is comparable with Fig. 5 showing identical offset misalignment at P2 for experiments 1, 3 and 4 and the differences in angular misalignment. Experiment 2 is purely angular but introduces some misalignment at the other measurement points.

Increasing rotation in Fig. 8 indicates an almost linear variation in misalignment. Small amounts of lead screw over/under rotation are responsible for the slight deviation.

Speed

The speed of the motor was also measured using LabVIEW. By monitoring distance over a 10 s period, shown in Fig. 9, the time for a full rotation was found. The magnified trace in Fig. 9 shows a cycle takes 1.3 s giving a speed of 46 rpm. This speed was appropriate to measure a temperature change on the rig and not exceed a motor temperature of 40 °C. By carrying out the measurement online, the method is validated and the variation in displacement of the shaft, the eccentricity, is also shown by Fig. 9. This 1 mm variation indicates that the shaft rotation is not perfectly true.

Temperature

The main aim of the experimental period was to detect and record temperature changes due to misalignment. The noncontact temperature measurement method was checked for its viability and investigated for future application. The direct and indirect effects of misalignment were found by respectively measuring the coupling closest to and furthest away from the rotated lead screw.

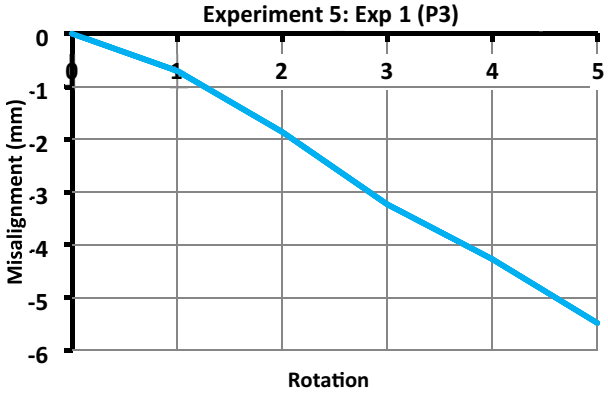

Fig. 8. Misalignment against rotation (left laser).

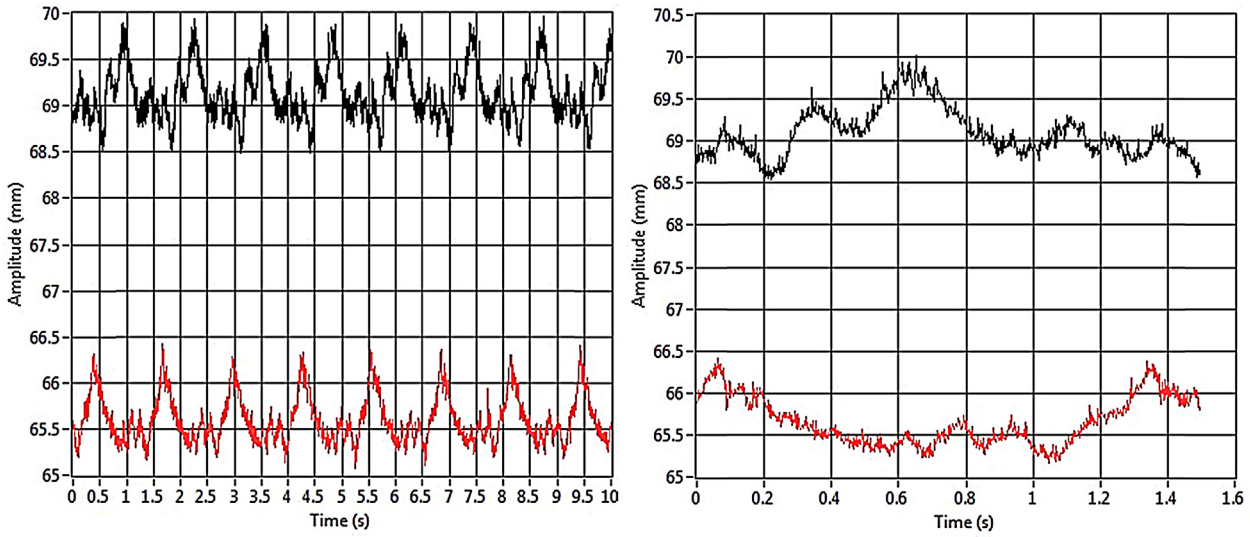

Fig. 9. Distance trace to calculate speed and magnified.

Varying misalignment

All varying plots were compared to entirely aligned and misaligned runs at similar ambient temperatures to reduce the likelihood of anomalous results. The common shape of the trace is seen in Fig. 10 with orange indicating the period of misalignment and ambient temperature in the figure reference. A temperature rise is evident when misalignment is introduced and a drop when the shaft is realigned. The size of the increase varies from experiment to experiment, for example, 2.36% for Fig. 10.

Since the offset introduced is identical for 3 experiments, the plots and percentage increases on coupling 1 are similar, at just over 2%. Lead screw 1 introduces this direct offset on coupling 1 and creates angular misalignment on coupling 2, seen in Figs. 5 and 11, with a rise of 2.59%.

However, this change does not correspond in reverse. Fig. 13 shows the minimal effect on coupling 1 that angular misalignment has, a change of only 0.84%. The largest increase of the varying experiments in Fig. 12 was 3.3%.

Offset is viewed as a larger increase in misalignment. Three rotations of lead screw one introduces offset directly to both couplings whereas the maximum angular misalignment is at the lead screw rather than the coupling. The angle introduced reduces the size of misalignment from 3 mm to 1 mm.

Both shaft and bearing displacement were evident due to misalignment, especially for experiments 3 and 4. The variation in coupling 2 is shown in Figs. 14 and 15, with a 2.33% increase evident in 14. However, in experiment 4 both lead screws are moved in the same direction, negating both angular misalignment and the offset created by coupling 1. Essentially, the shaft is

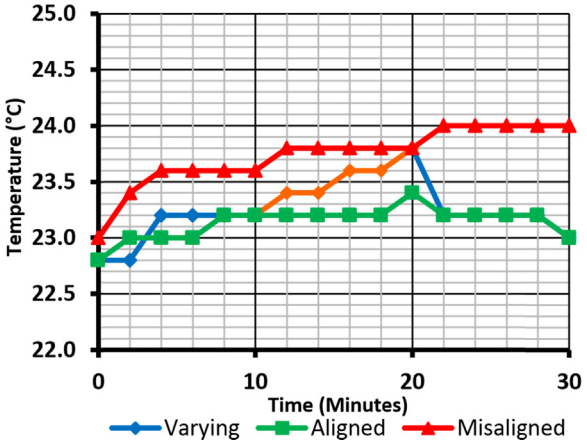

Fig. 11. Temperature plot – Exp 1 (C2) at 20 °C.

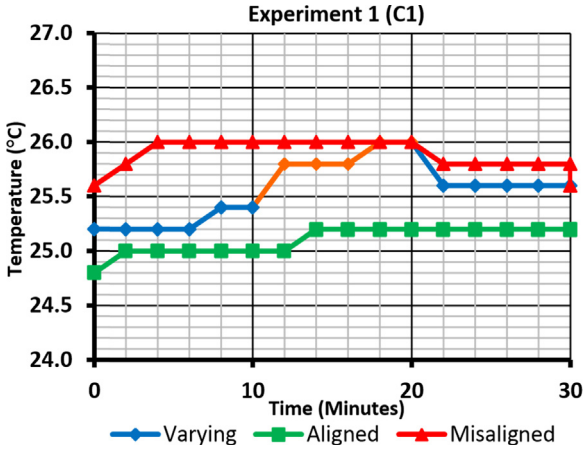

Fig. 10. Temperature plot – Exp 1 (C1) at 24 °C.

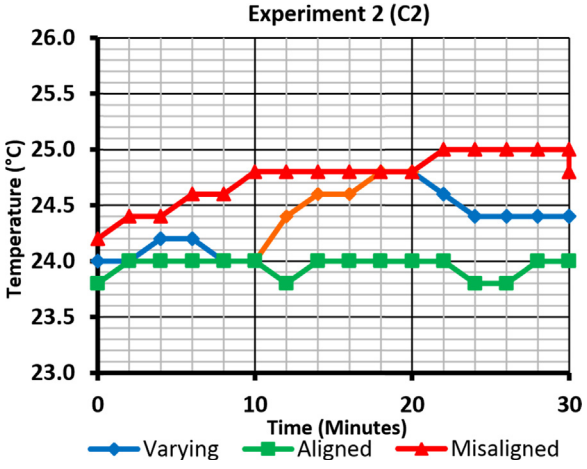

Fig. 12. Temperature plot – Exp 2 (C2) at 21 °C.

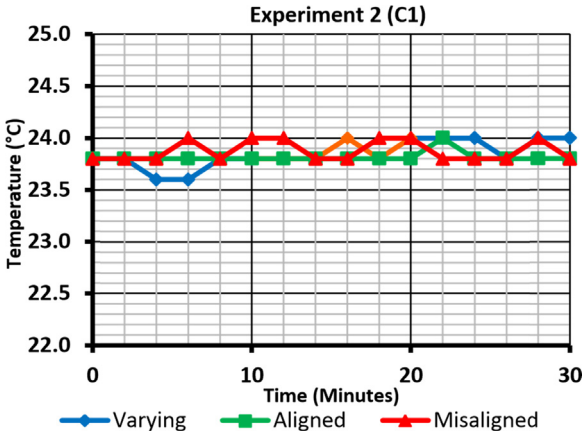

Fig. 13. Temperature plot – Exp 2 (C1) at 20 °C.

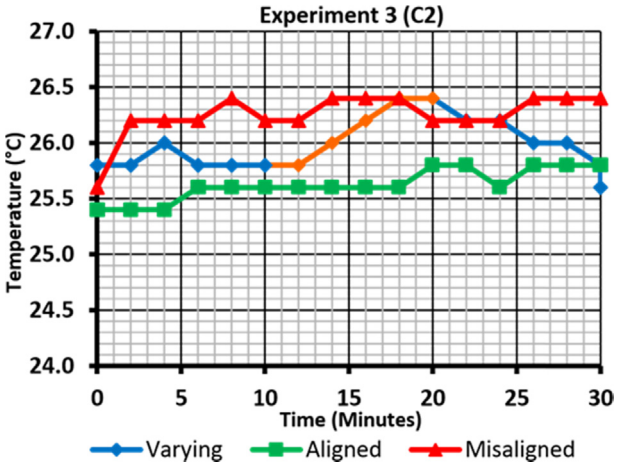

Fig. 14. Temperature plot – Exp 3 (C2) at 24 °C.

realigned with Fig. 15 indicating a small 0.83% rise on the second coupling.

Increasing misalignment

Experiment 5 was designed to show the differences in temperature rise between the four modes of misalignment. Direct comparisons are difficult to make between experiments 1–4 since ambient temperatures are not identical. Each run of experiment

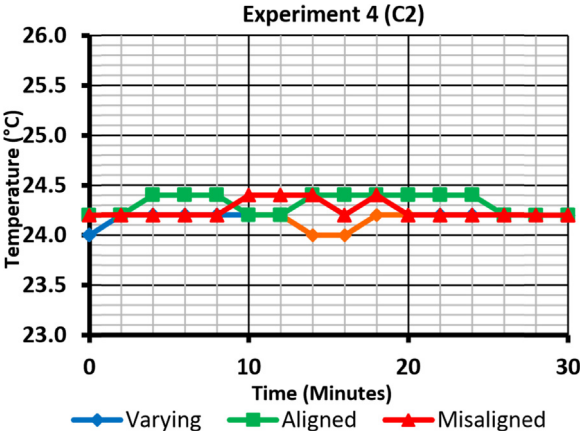

Fig. 15. Temperature plot – Exp 4 (C2) at 21 °C.

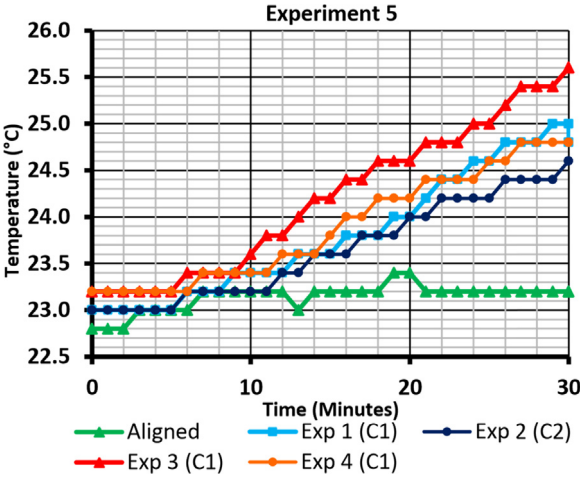

Fig. 16. Temperature plot – Exp 5 at 22 °C.

5 was carried out at an ambient temperature of 22 °C and compared to an aligned run to give greater strength to comparisons. The most severe temperature rise in Fig. 16 is 10.43% for experiment 3 where the system experiences the greatest amount of combined offset and angular misalignment. Experiment 2 – angular only – shows the smallest increase of 6.90% since the creation of angular is not as severe as offset. The percentage increase is much greater than the varying experiments since the amount of misalignment is increased to 5 rotations.

Ambient temperature

It was found that ambient temperature affected the measurement values significantly. Fig. 17 shows two aligned runs at fixed ambient temperatures which vary by approximately 4.8 °C. Letting the ambient temperature rise also highlighted the increase in monitored temperature.

Ambient temperature became a measured control point to distinguish between temperature rises due to misalignment or ambient temperature. Each experiment was additionally run at a different ambient temperature to ensure a similar temperature profile, seen when comparing Figs. 10 and 18 for Experiment 1 (C1). A rise of 1 °C is not unusual but at 18 °C creates a 5.15% increase, helped by the lower original temperature.

Operating temperature

The contribution of operating temperature was explored. Pre-running was used to reduce the sharp increase found in

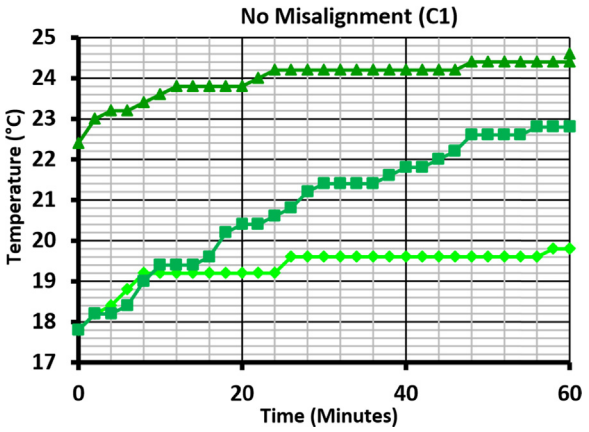

Fig. 17. Temperature plot of different ambient temperatures.

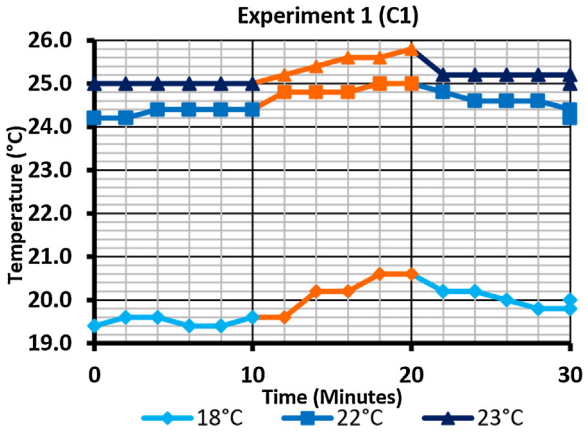

Fig. 18. Temperature plot – Exp 1 (C1) at different ambient temperatures.

preliminary experiments. However, there are still some slight increases evident in Figs. 10 and 11, for example.

Differences exist even though experiments were at identical ambient temperatures. Different starting temperatures were created by previous experimental runs. To ensure the starting temperatures were comparable, the rig was allowed to return to normal operating conditions before subsequent experiments.

Small temperature fluctuations are caused by the thermometer's display resolution of 0.2 °C. For example, if the temperature is hovering around 24.1 °C, 24.09 °C would display 24.0 °C and 24.11 °C would show 24.2 °C. Future investigations on a full size drivetrain should indicate the most suitable instrument and display resolution for temperature monitoring.

Discussion

The monitoring method indicated temperature rises due to the creation of misalignment as well as changes in ambient temperature and operating condition. The key is to distinguish which factor has caused the rise. The aim is to view the potential failure mode, the change due to misalignment, of which two types were analysed in this research. By taking ambient and nacelle temperatures into account evidence of misalignment can be found.

The designed monitoring method gathers data of temperature changes. This data, on an actual wind turbine, would be inputted into a SCADA system and root cause analysis incorporated using physics of failure. A temperature rise can be related through monitoring of other parameters such as transmission efficiency and rotational speed to detect and prognose fault development [8].

Causes of the temperature rise

Root causes of a temperature rise could be due to a change in ambient or operating conditions as studied in this research. On an actual turbine the ambient temperature will differ greatly and be much more variable than found indoors in this research.

Variation in ambient temperature causes the drivetrain to experience changes in operating temperature and can come from a number of areas. Location is one, since ambient temperature varies from country to country depending on the climate and time of day as well as position in terms of coastal or inland.

Misalignment has already been outlined as a more serious cause. Other reasons could be failure of a cooling system or components being run near their maximum capability. A turbine with greater power is likely to create higher temperatures, even if no fault or misalignment is present. Monitoring methods are required to be able to distinguish between the different contributory factors.

Effects of the temperature rise

Further investigations would be required into the effects of a temperature rise. This would be drivetrain and component specific so would be more appropriate on a full scale rig. The rig used in this research was sufficient for designing and validating the monitoring method.

Potential effects may have consequences for individual components such as couplings in terms of fatigue. Thermal ageing occurs when the component temperature is high enough – possibly due to overloading – to cause the material properties to degrade. Cycling of loading or temperature can also induce mechanical stresses causing deterioration and deformation, even if the temperature alone is insufficient to cause damage [15]. This fatigue is a process; cracks or wear increase until failure.

The overall system can be affected in terms of output. Maximising energy transfer is important within wind turbine systems. This transfer of energy, however, inevitably involves the dissipation of heat and therefore the loss of energy [15]. Investigations into energy loss due to misalignment vary in their results. Some report losses as high as 15% but an experiment similar in method to this research finds less than 3% [35]. Misalignment decreases torque so the amount of power transmitted through the shaft is reduced [39]. Should vibration arise, this leads to increased loading on components and reduces the operating life and efficiency. Cooling systems are used to reduce losses and wear due to overheating since maintenance due to fatigue or failure is a loss of availability.

Conclusion

This paper details the proposal and validation of a potential temperature monitoring technique for use in wind turbine condition monitoring. This non-contact method will aid fault detection at critical points.

Through the creation of misalignment, a temperature rise at the coupling mid-point was successfully detected using the technique. This analysis shows that misalignment is a direct cause of temperature change. A maximum temperature increase of approximately 5% was found from the varying experiments and above 10% in the increasing experiment. Further investigation found a rise in either ambient or operating temperature could also be detected. Through additional ambient temperature measurement the distinguishing factor can be uncovered.

Potential implications of a temperature increase, due to misalignment, have been discussed. These affect the couplings directly through fatigue and indirectly as a result of a loss of output. These are key focuses in terms of improving maintenance and reliability in a rapidly developing industry.

Both the technique and investigation require further development and research. The use of a handheld infrared thermometer was suitable for preliminary work but should be replaced with a fixed infrared thermometer, attached to a data logger, for more precise measurement. Results are always drivetrain specific so a full size rig is required to undergo experimentation, also enabling further investigations into the effects of misalignment.

Acknowledgments

The authors would like to acknowledge the finical support received from UK Engineering and Physical Sciences Research Council (EPSRC) Centre for Through-life Engineering Services

(EP/1033246/1, Project SC006) and EPSRC Impact Acceleration Award (EP/K50336811), Royal Academy of Engineering Newton Research Collaboration Programme (NRCP/1415/91) and Royal Society–National Natural Sciences Foundation of China International Exchanges Award (IE150600).

References

[1] Smolders, K., et al, 2010, Reliability Analysis and Prediction of Wind Turbine Gearboxes, European Wind Energy Conference (Warsaw), .
[2] UK Wind Energy Database, (2014), Available at:*http://www.renewableuk.com/en/renewable-energy/windenergy/uk-wind-energy-database/index.cfm*. (accessed 01.14.14).
[3] Tan, A., 2010, A Direct Drive to Sustainable Wind Energy, . Available at: http://windsystemsmag.com/article/detail/73/a-direct-driveto-sustainable-wind-energy (accessed 01.13.14).
[4] Wilkinson, M., et al, 2012, The Effect of Environmental Parameters on Wind Turbine Reliability, EWEA 2012 (Copenhagen), .
[5] Wilson, G., McMillan, D., 2014, Assessing Wind Farm Reliability Using Weather Dependent Failure Rates,Conference Series 524 – The Science of Making Torque From Wind. Journal of Physics, 012181.
[6] Wilson, G., McMillan, D., 2014, Quantifying the Impact of Wind Speed on Wind Turbine Component Failure Rates, Proc. Eur. Wind Energy Conf. (Barcelona, Spain, March 10–13), .
[7] Carroll, J., McDonald, A., McMillan, D., 2015, Failure Rate, Repair Time and Unscheduled O&M Cost Analysis of Offshore Wind Turbines, Wind Energy, .
[8] Whittle, M., et al, 2013, Improving Wind Turbine Drivetrain Reliability Through Pre-Misalignment, Wind Energy, 17/8: 1217–1230.
[9] Faulstich, S., et al, 2011, Wind Turbine Downtime and Its Importance for Offshore Deployment, Wind Energy, 14/3: 327–337.
[10] Tavner, P.J., 2012, Offshore Wind Turbines: Reliability, Availability and Maintenance, The Institution of Engineering and Technology, London.
[11] Garrad Hasan, G.L., 2013, Offshore Wind – Operations and Maintenance Opportunities in Scotland – An Insight Into Opportunities, .
[12] Available:In: *http://www.scottishenterprise.com/~/media/SE/Resources/Documents/MNO/Offshore%20wind%20operations%20and%20maintenance%20opps.pdf*. (accessed 01.15.14).
[13] Dinwoodie, I., McMillan, D., Revie, M., Lazakis, I., Dalgic, Y., 2013, Development of a combined Operational and Strategic Decision Support Model for Offshore Wind, Proc. Deep Wind Conf. (Trondheim, Norway, January 24–25), .
[14] Van Bussel, G.J.W., Zaaijer, M.B., 2001, Reliability, Availability and Maintenance – Aspects of Large-Scale Offshore Wind Farms, A Concepts Study, MAREC 2001 (Newcastle), .
[15] Mobley, R.K., 2004, Maintenance Fundamentals, Elsevier Butterworth-Heinemann, Oxford.
[16] Tavner, P.J., et al, 2008, Condition Monitoring of Rotating Machines, The Institution of Engineering and Technology, London.
[17] McMillan, R.B., 2004, Rotating Machinery: Practical Solutions to Unbalance and Misalignment, Fairmont Press, Lilburn.
[18] Hariharan, V., Srinivasan, P.S.S., 2009, Vibration Analysis of Misaligned Shaft-Ball Bearing, Indian Journal of Science and Technology, 2/9: 45–50.
[19] Neale, M., et al, 1998, Couplings and Shaft Alignment, Arrowhead Books.
[20] Patel, T.H., Darpe, A.K., 2009, Experimental Investigations on Vibration Response of Misaligned Rotors, Mechanical Systems and Signal Processing, 23/7: 2236–2240.
[21] Vance, J.M., 1988, Rotordynamics of Turbomachinery, Wiley.
[22] Kim, S.M., et al, 2009, A Smart Memory Type of Data Acquisition System for Shaft Misalignment Maintenance, Journal of Mechanical Science and Technology, 19/1: 15–27.
[23] Simm, A., Wang, Q., Huang, S.L., Zhao, W., 2016, Laser Based Measurement for the Monitoring of Shaft Misalignment, Measurement, 87:104–116.
[24] Talbot, J., Wang, Q., Brady, N., Holden, R., 2015, Offshore Wind Turbine Blade Measurement Using Coherent Laser Radar, Measurement, 79:53–65.
[25] Fulzele, A.G., et al, 2012, Condition Monitoring of Shaft of Single-Phase Induction Motor Using Optical Sensor, Mechanical Systems and Signal Processing, 29:428–435.
[26] McMillan, D., Ault, G.W., 2007, Quantification of Condition Monitoring Benefit for Offshore Wind Turbines, Wind Engineering, 31/4: 267–285.
[27] Feng, Y., Tavner, P.J., 2010, Introduction to Wind Turbines and Their Reliability & Availability, SUPERGEN Wind EWEC2010 Side Event (Warsaw), .
[28] Siemens, A.G., 2011, Reliable Connections – Flender Couplings, .
[29] Simm, A., 2013, Monitoring of Shaft Misalignment Using Laser Based Measurement Methods (Technical Report), Durham University School of Engineering and Computing Sciences.
[30] Available:In: *http://www.industry.usa.siemens.com/verticals/us/en/oilgas/Documents/Couplings_Reliable_Connections.pdf*. (accessed 17.03.14).
[31] Mohanty, A.R., Fatima, S., 2015, Shaft Misalignment Detection by Thermal Imaging of Support Bearings, in: Proceedings of International Federation of Automatic Control Conference, pp.554–559.
[32] Cengel, Y.A., Boles, M.A., Kanoglu, M., 2011, Thermodynamics: An Engineering Approach, 7th ed. McGraw-Hill.
[33] Incropera, F.P., DeWitt, D.P., 2006, Fundamentals of Heat and Mass Transfer, 6th ed. John Wiley & Sons.
[34] Manwell, J.F., et al, 2009, Wind Energy Explained, John Wiley & Sons Ltd, Chichester.
[35] Hodowanec, M., 1997, Effects of Coupling Installation on Motor Performance, IEEE Industry Applications Magazine, 70–77.
[36] Yang, W., et al, 2008, Wind Turbine Condition Monitoring and Fault Diagnosis Using Both Mechanical and Electrical Signatures, AIM 2008 Xian, .
[37] Gaberson, H.A., 1996, Rotating Machinery Energy Loss Due to Misalignment, in: Proceedings of the 31st Intersociety Energy Conversion Engineering Conference (Washington, DC), .
[38] Tavner, P.J., 2008, Review of Condition Monitoring of Rotating Electrical Machines, IET Electric Power Applications, 2/4: 215–247.
[39] Zocholl, S.E., 1990, Motor Analysis and Thermal Protection, IEEE Transactions on Power Delivery, 5/3: 1275–1280.